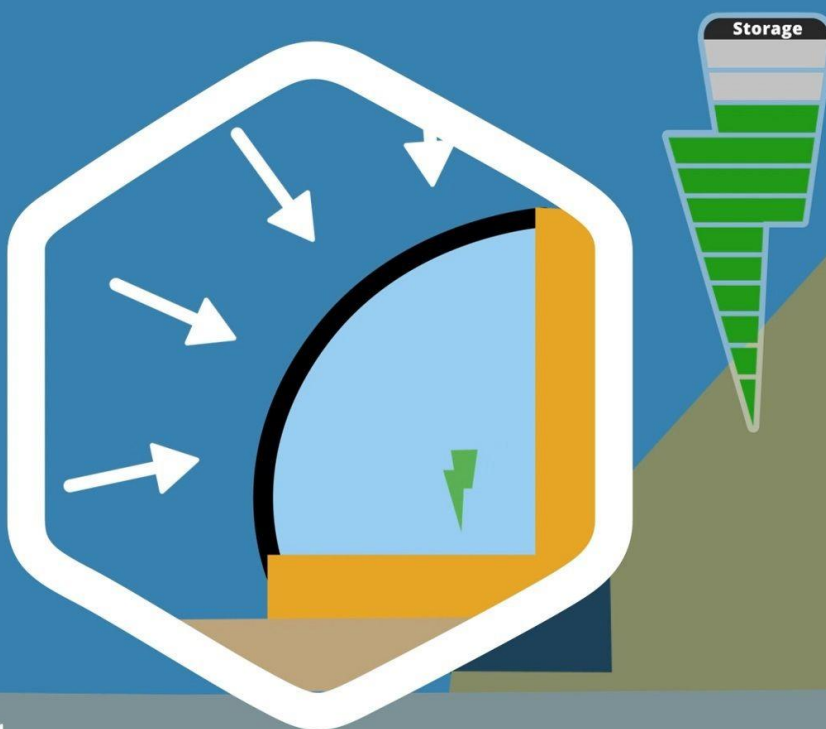


Flexible Membrane Deformation: Simulation Optimization and Analysis

Philippe A. Tarjan

S2941791



Integration Project [Block II, 2019]

1st Supervisor: A. Vakis

2nd Supervisor: A. Geertsema

Abstract

The Ocean Grazer uses an underwater flexible reservoir to store potential energy. The bladder is filled with excess energy and when the bladder discharges, an electric turbine is turned. Little is known about the deformation behavior of a discharging bladder, so simulations were made. The current simulations and behavior analysis of the flexible bladder are oversimplified and are not yet considered to be fully optimized; for example, the hydrostatic pressure gradient is not captured by the current simulation. This project aims to optimize the simulations and analyze the deformation behavior during bladder discharge.

Table of Contents

Abstract.....	2
Research and Design Topic	4
Problem Analysis.....	4
System.....	4
Stakeholder(s)	6
Problem Statement.....	7
Research Goal	8
Methods.....	8
Literature Review.....	9
Membrane Geometry	9
External Environment	10
Risk Analysis.....	11
State of the Art.....	12
Domain(s).....	12
In/Outflow.....	12
Boundary Constraints	13
Adding Working Principles	14
Pressure-based Outflow.....	14
Hydrostatic Pressure Gradient.....	16
External Flow.....	20
Reverse Boundary Spring Load	23
Further Analysis	27
Membrane Thickness.....	28
Membrane Geometry	31
Discussion & Implications	33
Summary	35
References	37
Appendix	38
A. Working Principle: Hydrostatic Pressure Gradient	38
B. Further Analysis: Membrane Geometry	39
C. Optimality.....	41

Research and Design Topic

The Ocean Grazer is a new offshore renewable energy harvesting concept developed by the University of Groningen. Its goal is to capture energy from the wind and waves and have the capability to supply this energy at any time, specifically when there is demand for it. Ocean Grazer seeks to obtain this by incorporating an on-site energy storage system, which takes the shape of an over-pressured flexible bladder capable of storing potential energy. This bladder is located deep underwater at the base of the wind turbine and is pumped full of water when there is an excess of energy or a low demand for energy. When this potential energy is desired, a valve opens within the bladder and the hydrostatic pressure and over-pressure (due to membrane stretching) force the water through a small electrical turbine.

COMSOL simulations of the flexible reservoir have been commissioned in the past. These simulations are however not fully optimized. The output of this research paper will be an 'optimal' COMSOL simulation, based on criteria defined in 'Research Goal', as well as further analysis of the deformation behavior.

Problem Analysis

System

In *fig. 1*, the most current design of the pump storage system of the Ocean Grazer can be observed.

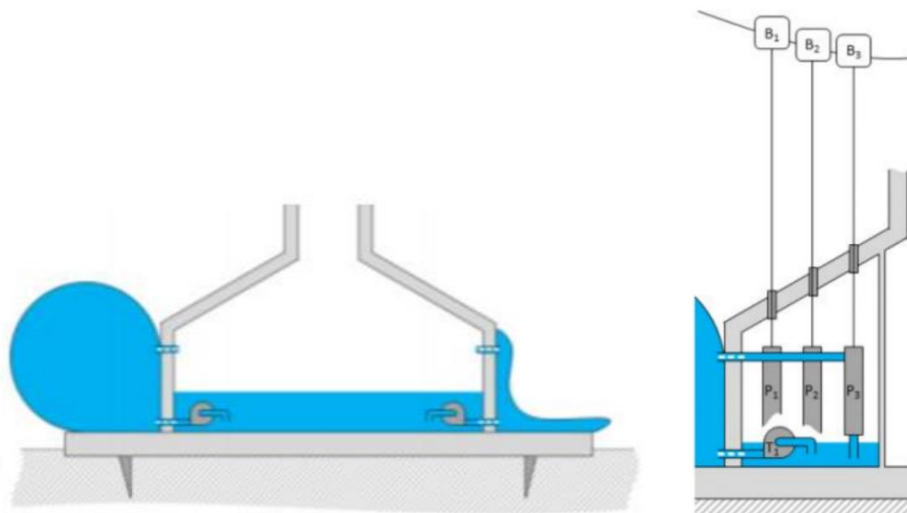


Figure 1 (Elzen, 2018)

The energy storage system works by using the mechanical energy supplied by waves to operate pistons (Vakis, 2015). These pistons draw water out of the rigid reservoir tank, and into the flexible bladder. The current inlet into the flexible bladder is found towards the top of the bladder, and the outlet can be found towards the bottom of the bladder. The internal working fluid inside the system is currently assumed to be fresh water (Rooij, 2019). Furthermore, the material (EPDM) of the flexible bladder is assumed to be a hyper-elastic in nature.

When the liquid is pumped out of the rigid reservoir and into the bladder, the pump must overcome the surrounding hydrostatic pressure. This means once the water is inside the flexible reservoir, the pressure inside the flexible reservoir will equal that of its surrounding environment. Because the rigid reservoir is connected to the surface and is therefore at atmospheric pressure ($1 \text{ [atm]} = 101000 \text{ [Pa]}$), a pressure differential between the flexible bladder and rigid reservoir exists. When this stored mechanical potential energy is released via the outlet, a small turbine converts the mechanical energy into electricity and this electricity is then send to the main grid via underwater cables.

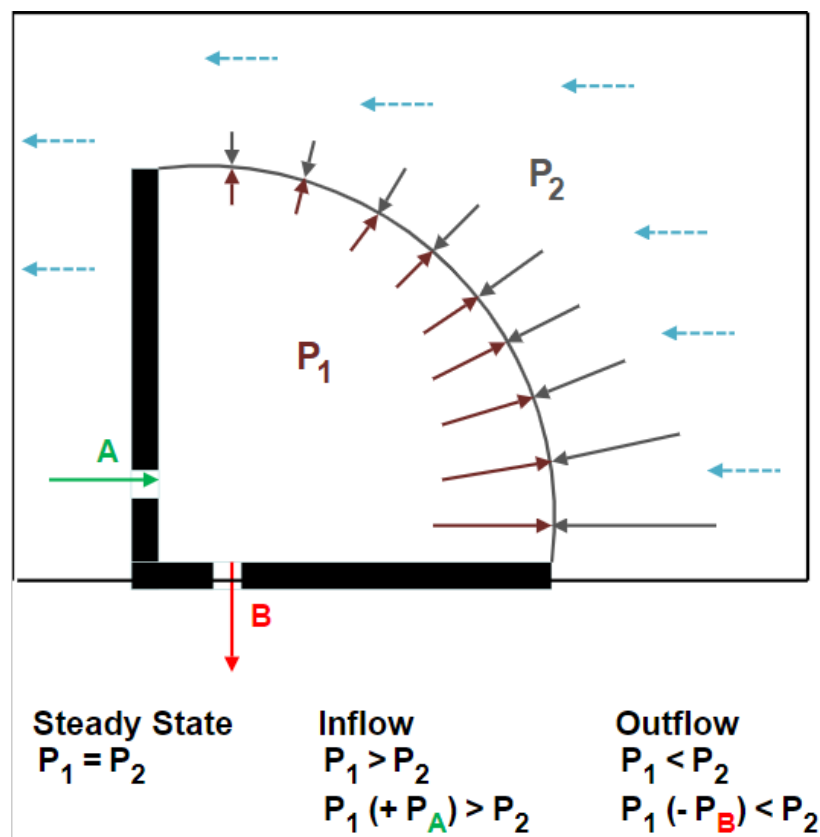


Figure X: System Description

Fig. X helps define the system and its environment. The blue dashed arrows represent the flow of an underwater current, while the gray arrows represent the force exerted by the hydrostatic pressure gradient. It is important to note that the hyper-elastic flexible membrane can be stretched past its “steady-state” position, if steady-state is defined as the position the membrane is in while fully filled but *not* stretching past its initial length. Stretching the membrane will create overpressure within the bladder as the stretched membrane exerts a spring force. This won’t miraculously create extra potential energy out of nothing however; this spring force must first be overcome during the pumping mechanism, meaning that a pumping pressure greater than that of the surrounding hydrostatic pressure will be necessary to fill the bladder past steady state. Overpressure will not be considered in this project, as the focus of the research conducted is on the discharge of the bladder.

In order to better understand and predict the behavior of the flexible bladder deformation process, simulations of the system have been commissioned by Ocean Grazer. These simulations have been designed by Sietse van den Elzen using COMSOL. The current model is based off a 2D slice taken from a 3D COMSOL model of the system, as running simulations using the 3D model would be too computationally expensive (Elzen, 2018). The current 2D model is simulated using a fluid-structure interaction Multiphysics interface, using an arbitrary Lagrangian-Eulerian method to combine the spatial frame (with solid mechanics) and fluid flow (with Eulerian description). A more detailed description of the current simulation model will be discussed in the ‘State of the Art’ section.

Stakeholder(s)

The problem owner is Marijn van Rooij (CTO & Research Leader of Ocean Grazer B.V.). Mr. van Rooij has a great deal of interest in the realization of a simulation that mimics the real behavior of the flexible bladder as closely as possible, because as the CTO of Ocean Grazer B.V., he is striving towards the actualization of this research project on a commercial scale. It is in Mr. van Rooij’s best interests to be able to predict the performance of the potential energy storage system accurately as once the final design is realized and physical full-scale tests are carried out, it will be more expensive to rework any design flaws (Anderson, 2002). Mr. van Rooij also has the greatest degree of influence on the research conducted, as he will assist in decision making

regarding which variables are relevant and which can be safely ignored, therefore having a direct impact on the output of the research.

Antonis Vakis (Research Staff Ocean Grazer UG) must also be considered a stakeholder as he not only is part of the research staff of Ocean Grazer UG, but also is this Bachelor IP's project supervisor. Prof. Vakis has an interest in the output of this Bachelor IP, as he must find the level of research done satisfactory to warrant a passing grade, as well as ensure that the research conducted is relevant to improving the design of the Ocean Grazer. Furthermore, W.A. Prins (Research Manager Ocean Grazer UG) has a great deal of interest in the realization of a simulation that mimics reality closely because as the inventor and former research manager, he has the responsibility and the motivation to conduct research in the most comprehensive way possible.

Problem Statement

The current fluid-dynamic simulations of the deformation behavior of the flexible membrane may not be optimal. For example, the movement of the membrane is currently assumed to be a product of the in- and out- flows (Rooij, 2019). In reality the in- and out- flows result from the inflation and deflation of the bladder due to the pressure differential between the flexible and rigid reservoir and the surrounding hydrostatic pressure gradients. Additionally, external variables that will influence the deformation process are not yet included in the current simulation. For example, an underwater current may have some effect on the system, as well as the pressure gradient in the surrounding water, and these (among other factors) are currently missing from the simulation.

Furthermore, further analysis of the deformation process is not yet comprehensive. For example, the current fluid-dynamic simulations suggest that problems arise when fully deflating the flexible membrane (Elzen, 2018). The membrane blocks the outflow pipe during discharge, and it is thus not possible to completely discharge the pipe. This wastes potential energy and reduces the overall efficiency of the Ocean Grazer. Additionally, no analysis has been done on the effect of varying the membrane geometry on the deformation process (Vakis, 2019); it is reasonable to assume that the flexible membrane will behave differently given diverse membrane thickness and/or shape.

Research Goal

The research goal of this research project is to *optimize the COMSOL simulation & preform further analysis of the flexible bladder reservoir*. This will be done by first improving the existing model by updating the relevant physics, then adding the influence of its external environment (such as hydrostatic pressure gradients and underwater currents), and then eventually carrying out further analysis on the deformation behavior based on membrane geometry. Efficacy of the eventual output of this research (updated model & further testing) will be evaluated by assessing the simulation's optimality. "Optimal" will be defined as the simulation model's ability to reliably model the deformation behavior (with respect to its external environment). This can be quantified as the computational time needed to run said simulation, and the accuracy of the model with respect to the relevant physics.

In order to realize this research goal, the following research questions must be answered:

- *How is current system modelled? Which assumptions have been made? How can the relevant physics incorporated in the current model be amended?*
- *What does its typical external environment consist of (that has the potential of influencing the membrane deformation behavior)?*
- *How does varying membrane geometry influence the deformation behavior?*

Methods

The system of approaching this research project is the regulative cycle. The regulative cycle consists of 4 parts;

Analyze: The current model & simulations of design are studied. Literature is reviewed to gain more knowledge about similar processes & their simulations. Interviews with stakeholders are conducted. Through this, expectations of future design are determined.

Design: A new model is designed, given the output of the analysis. The model will be designed in a way that aims to determine relevant variables/working principles.

Develop: The design is now combined with operational information and modelled in COMSOL given the variables desired in this turn of the regulative cycle.

Implement: The results of the simulation are compared to the desires of Ocean Grazer B.V., and hopefully after multiple iterations, a clear superior design evolves.

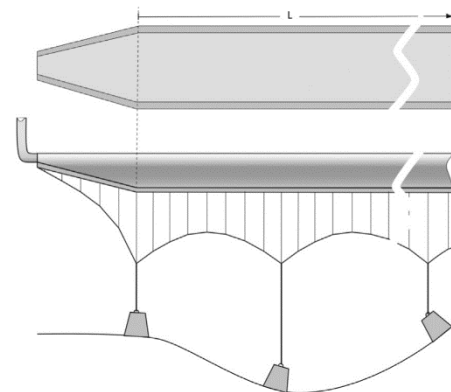
Literature Review

Membrane Geometry

UWCAES stands for Underwater Compressed Air Energy Storage. These systems operate in a similar way to the Ocean Grazer's potential energy storage system; a flexible bladder is filled with air (in the Ocean Grazer's case water) underwater and when the energy is required, a valve in the bladder allows the surrounding hydrostatic pressure to deflate the bladder. Though this article focuses on air storage systems and not water, the similarity of the working principles between the two designs allow for relevant information to be covered.



Standard UWCAES (Mas, 2016)



Tubular UWCAES (Mas, 2016)

The focus of the article is not on the general system of an UWCAES, but rather on the geometry of the flexible bladder. The author, Javier Mas, proposes a tubular design of the flexible membrane rather than the spherical design UWCAES currently have (Mas, 2016). Please note that when viewed as a 2D slice, the tubular design evokes a rectangle, whereas the spherical design evokes a circle. The images found above help exemplify the traditional design (left) versus a tubular design (right). The benefits of having a tubular design are as follows. The structural simplicity is increased,

reducing cost to manufacture (Mas, 2016). The scalability is improved as well, as there is now a means of extending the system (lengthwise) without needing to replicate all the components.

It isn't nonsensical to assume that the benefits experienced by a tubular UWCAES will also benefit the design of the Ocean Grazer's flexible reservoir. It is important to note that air is significantly less dense than water, meaning that an UWCAES will be much more buoyant than of the Ocean Grazer's flexible reservoir (as water vs. seawater yields a much smaller density differential). The implementation of a tubular (2D slice = rectangular) design for the Ocean Grazer's membrane will be explored in "further analysis".

External Environment

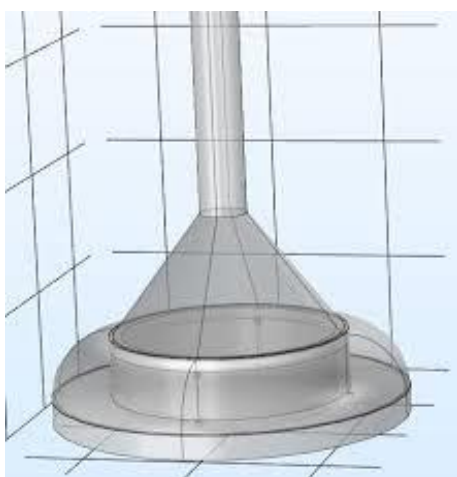
In order to determine which range of external flow rates the Ocean Grazer's flexible reservoir could experience, a literature search was conducted. Two factors are responsible for the generation of ocean currents; the wind and water temperature differential. The effect of the wind on ocean currents is relevant until approximately 100 [m] of depth (Gordon, 2018). The temperature differential between different horizontal layers of ocean water lead to a water column becoming unstable, leading to thermohaline circulation (Augustyn, 2018). Thermohaline circulation is defined as density-dependent currents. The density differential exists as a result of the temperature delta leading to a rate of evaporation delta, and eventually a difference in salinity between ocean water layers (C.D. de Jong, 2010). The flow rate of these currents varies depending on geographic location, and current generally diminishes in intensity with increasing depth.

In order to prepare the primary stakeholder for the implementation of the Ocean Grazer's flexible reservoir anywhere around the world, the simulation must be able to model a horizontal flow rate maximum of 4 [m/s] and a minimum of 0.004 [m/s] (Gordon, 2018). The vertical flow rates ("up/down welling") are very slow, at an average rate of 1 [meter/month] (Gordon, 2018). Because of this, the vertical flow rates will be ignored.

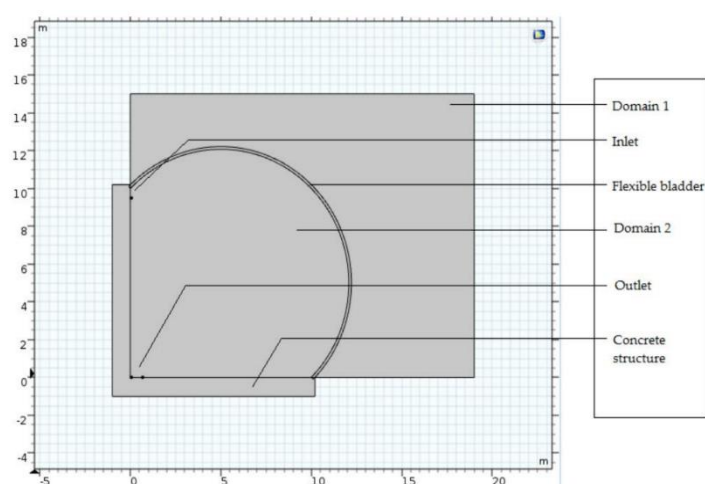
Risk Analysis

The inherent risk of this research design plan comes in the form of efficacy of output to Ocean Grazer B.V., as well as the ability to reliably make conclusions about simulation model's optimization.

The simulation model is currently a 2D slice of a larger 3D system. This simplification of reality has significant ramifications with respect to the relevance of the conclusions drawn from this research project. Because a 3D surface deforms differently than a 2D surface (Geertsema, 2019), information about the membrane's exact position at a given time cannot be taken as fact but should be something closer to a guideline of how the membrane will deform. Furthermore, when the simulation is being evaluated on its ability to predict how the bladder will work, assumptions must be made in order to compare its output data to what we expect to happen in reality. A down-scaled physical test model has been built in the past, but this physical test model was set in a static hydrodynamic environment (no underwater currents) and was not subjected to hydrostatic pressure. Because of these key differences, comparisons between the deformation behavior of the test model and the simulation model will not help us reach a more optimal output simulation. The "closeness" of the eventual output simulation's behavior to that of a full-size physical model must also be inferred based upon the existing knowledge base of hydrostatic pressure gradients and hyper-elastic materials, potentially leading to human error and/or confirmation bias.



Original Model A: 3D Render (Elzen, 2018)



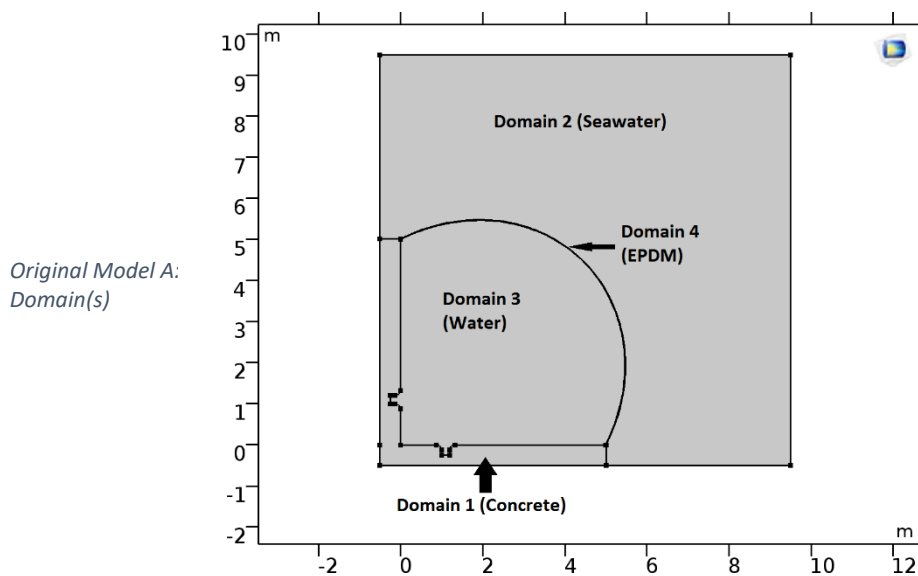
Original Model A: 2D Slice (Model) (Elzen, 2018)

State of the Art

‘Original Model A’ is the most current and optimal simulation model (at the start of this research). In this section, the boundary conditions and parameters of the ‘Original Model A’ will be analyzed, in order to better understand the changes made in order to realize the research goal.

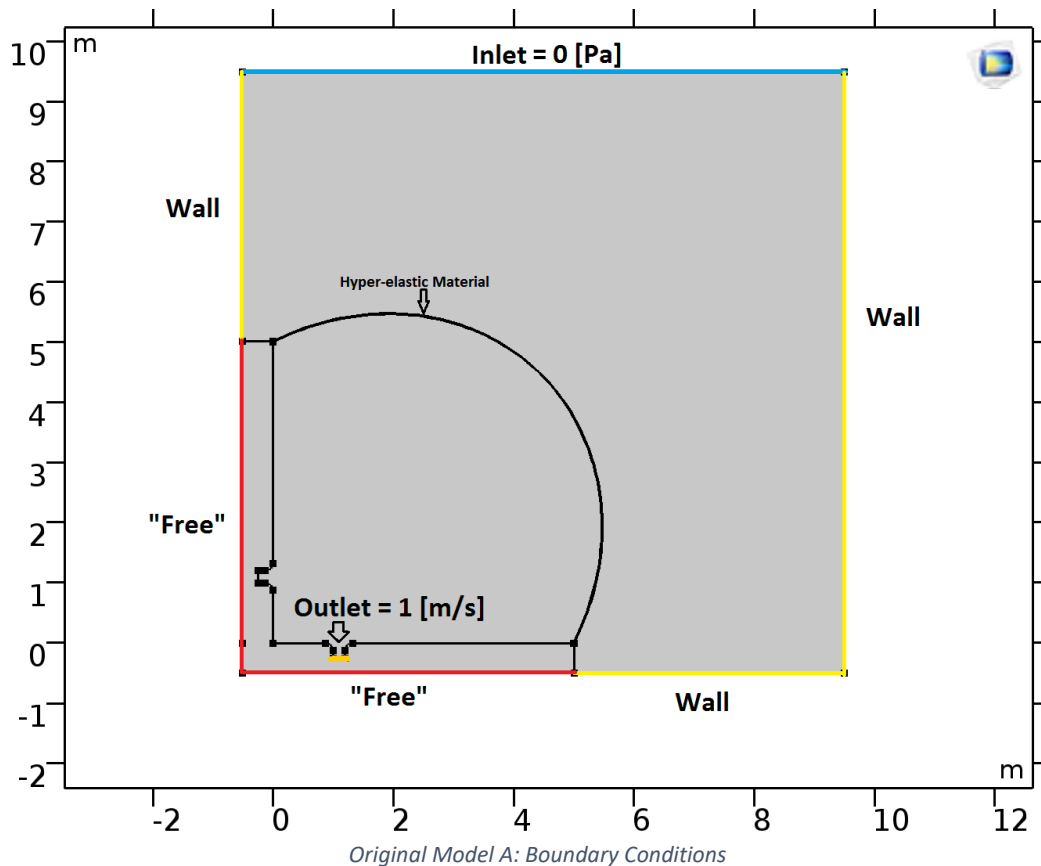
Domain(s)

The ‘Original Model A’ has 4 distinct domains, as seen above. Domain 1 captures the fixed structure holding the membrane in place and is assigned the material Concrete. Domain 2 captures the liquid surrounding the membrane and is assigned the custom material Seawater. Domain 3 captures the liquid encased by the membrane and is assigned the material Water. Domain 4 captures the flexible membrane and is assigned the hyper-elastic material EPDM. All Domains and materials will remain unchanged in updated versions of the ‘Original Model A’.



In/Outflow

The Outlet boundary of the ‘Original Model A’ is located along the horizontal plane of the concrete structure, offset slightly to the left. The Inlet boundary (located on the vertical plane) will be ignored, as this research project focuses on only the deformation of the bladder during discharge. The Outlet boundary has been prescribed a normal outflow velocity, smoother with a rectangular function and having a maximum velocity of 1 [m/s]. The prescribed normal outlet flow *pulls* (rather than *pushes*) the volume of water out of the bladder, resulting in the deformation of the membrane.



Boundary Constraints

The top boundary is currently modelled by an outlet with Pressure condition of 0 [Pa]. This allows for water to enter the system when there is flow through the bladder outlet (which creates a negative pressure within the system). Both side and bottom boundaries are modelled by walls which prevent the in or outflow of liquid over these boundaries. Along the outside of the cement walls, the “Free” boundary condition is assigned so that the cement structure is fixed in place and that no Fluid-Structure Interaction can occur along this boundary. Domain 1 (concrete) is set to be a “Fixed Constraint”, meaning that it is assumed that this structure is immovable and will not deform in any way during the filling or discharge of the bladder. The flexible bladder is explicitly defined as a hyper-elastic material, described by the Neo-Hookean material model with the assumption of a nearly incompressible material.

Adding Working Principles

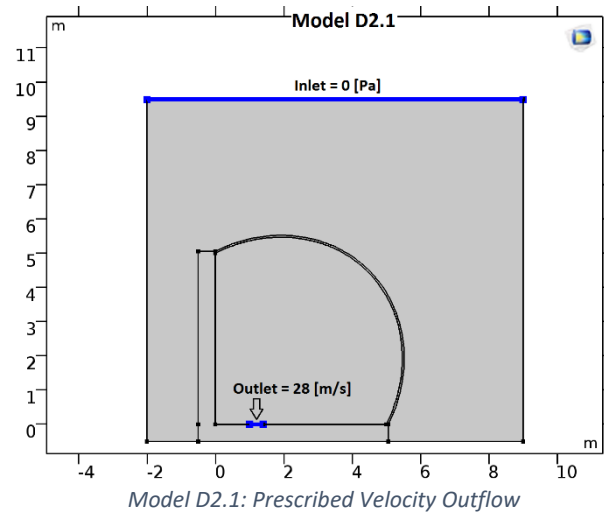
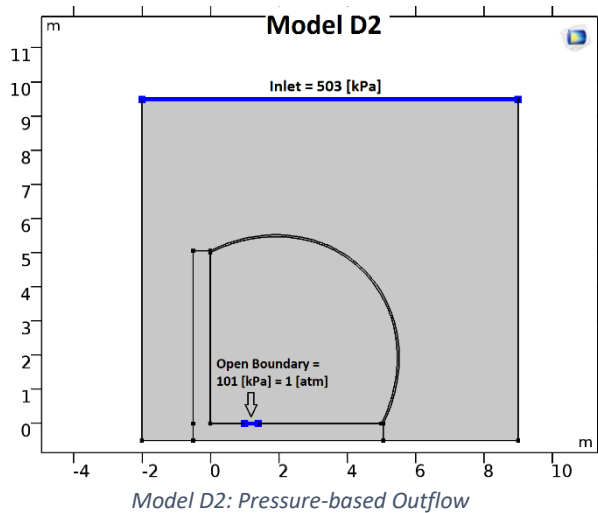
In order to optimize the bladder deformation simulations, assumptions made in the ‘Original Model A’ will be replaced with boundary conditions that more accurately represent the physical phenomena within the system. Every new addition to the simulation model will be represented by working principles. Each one of these working principles is meant to add relevant complexity and will be analyzed in terms of efficacy to the research goal of creating a more optimal simulation model. The *figure Y* below helps organize the findings of the ‘Adding Working Principles’ section, as well as give the reason why a working principle is included in the ‘Final Model A’. (Appendix C)

		Model Validity	Influence on Deform. Behavior	Reduce Computational Expense	= Optimality	FINAL MODEL
Working Principles	Pressure-based Outflow	2	1	0	3	X
	Hydrostatic Pressure	2	2	-1	3	X
	External Flow	2	2	-1	3	X
	Reverse Loading	-1	1	-1	-1	

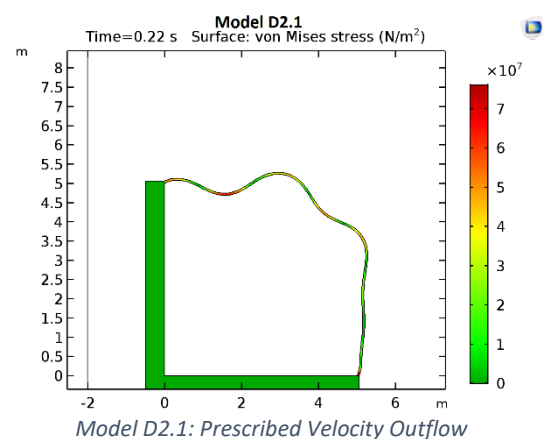
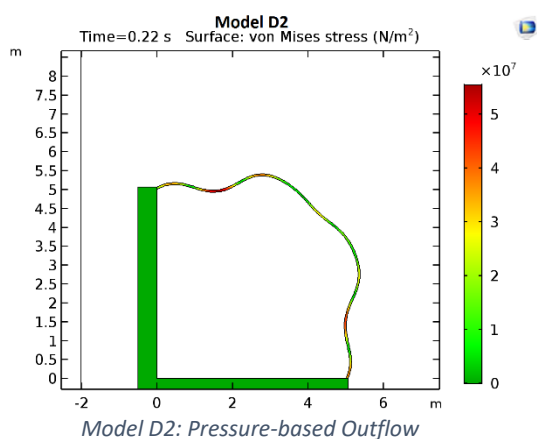
Figure Y: Values = assigned weight of correlation with range $\in [-2,2]$
MORE INFO: Appendix C

Pressure-based Outflow

As previously mentioned, the ‘Original Model A’ sets a prescribed velocity along the boundary of the Outlet. This in turn *pulls*, rather than *pushes* the water through the Outlet. In reality, this is not what happens; the bladder is discharged due to the pressure differential between the water inside of the membrane and the pressure in the fixed reservoir. Because the flexible reservoir is open and connected to the surface, the pressure inside will be equal to 1 [atm]. In order to replicate this state within the simulation, an “Open Boundary” condition is assigned to the Outlet, with a pressure of 1 [atm]. This allows for the outflow velocity and deformation behavior of the membrane to be dependent on the pressure differential between the hydrostatic pressure and the atmospheric pressure, meaning that results that more accurately reflect reality can be expected.



In order to evaluate the efficacy of this working principle, the deformation behavior of the membrane is analyzed between two nearly identical models ('Model D2' and 'Model D2.1'), with the only difference between them being the way outflow is described. In 'Model D2', the outflow is pressure-based and the outflow velocity over time is recorded. In 'Model D2.1', the outflow is prescribed to be the average velocity obtained in 'Model D2'. As seen in the images below, the way the membrane deforms due to a pressure-based outflow versus the way the membrane deforms due to a prescribed velocity are significantly different; in 'Model D2.1' (prescribed outflow) the flexible membrane initially deforms near the highest point of the bladder, whereas in 'Model D2' (pressure-based), the initial deformations occur simultaneously at the top and bottom. This difference in behavior implies that adding this working principle to the eventual output model is worth the extra computational expense, as using a prescribed velocity outflow will lead to unreliable results. Furthermore, if the outflow velocity between different models needs to be compared, this can only be done if the outflow velocity is a dependent variable. For these reasons, all further models will be assigned a Pressure-based Outflow.



Hydrostatic Pressure Gradient

Now that a pressure-based outflow has been assigned to the model, it is necessary to create the pressure differential between the fixed and flexible reservoirs. In reality, this pressure differential is created by the hydrostatic pressure gradient of the surrounding seawater (Domain 2), applying a normal force over the area of the flexible membrane. The formula for the hydrostatic pressure at a given depth is captured by the following equation (Frei, 2014):

$$P = \rho g z + P_0$$

where

P is the Pressure

ρ is the density of the surrounding liquid,

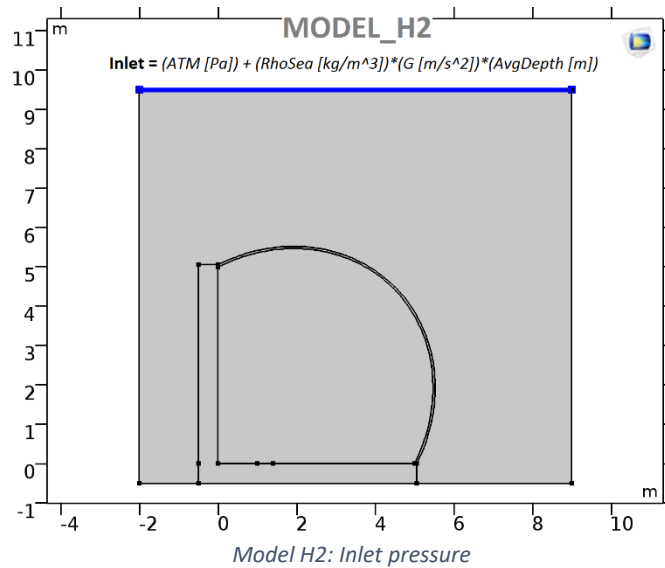
g is the gravitational constant, and z is the depth from surface

P_0 is the pressure at the surface (1 atm)

In order to determine the optimal way of modelling the hydrostatic pressure, 3 separate models have been created. ‘Model H2’ has the same pressure-based outflow modelled in the previous section. In order to emulate the pressure exerted on the system, a pressure-based Inlet is assigned to the entire top boundary edge of Domain 2 (Seawater). The function is equal to

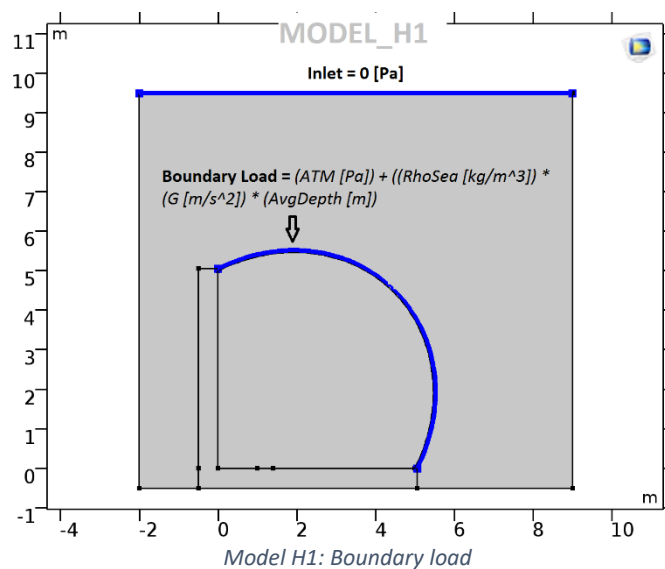
$$P = (ATM [Pa]) + (RhoSea [kg/m^3]) * (G [m/s^2]) * (AvgDepth [m])$$

The variable $AvgDepth = Depth + (h1/2)$, where $h1$ represents the height of the concrete structure. $RhoSea$ and G are the density of Seawater and the gravitational constant, respectively. This ensures that the average hydrostatic pressure (given the depth) is applied from the top of the system downwards.



However, when looking at the system description (*fig. X*, 'System') and the definition of hydrostatic pressure, it becomes clear that this inflow pressure models the hydrostatic pressure gradient in the wrong way. Hydrostatic Pressure is a normal force that acts perpendicular to the surface of the object it is acting on, whereas the pressure set in 'Model H2' simply works downwards along the y-axis.

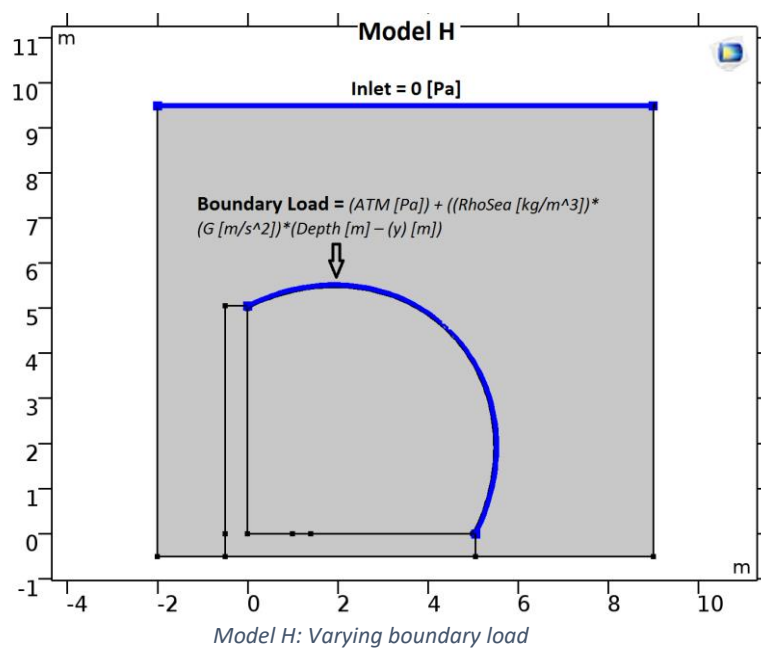
'Model H1' attempts to apply a perpendicular force to the flexible membrane by setting a "Boundary Load" over the outside edge of the flexible membrane domain. The same function used in 'Model H2's Pressure-Based Inlet is utilized (with *AvgDepth*). The top boundary (of Seawater) is kept as a Pressure-based Inlet but because the applied Boundary Load is modelling the hydrostatic pressure, the pressure at the top boundary is set equal to zero. This ensures that water can be pulled into the system while it is being pushed out of the outflow, but no extra load will be applied because of this action.



Though assigning these boundary conditions brings the simulation closer to system described by *figure X*, it is still assuming that the hydrostatic pressure doesn't change with depth, which is fundamentally incorrect. As seen in *fig. X*, the gray arrows representing the force exerted by the hydrostatic pressure gradient increase in length the deeper the membrane is, implying that the force increases as depth increases.

In order to model this phenomenon in the simulation and still maintain the direction of the force (modelled in 'Model H1'), a new 'Model H' is created with the boundary load pressure function changed to

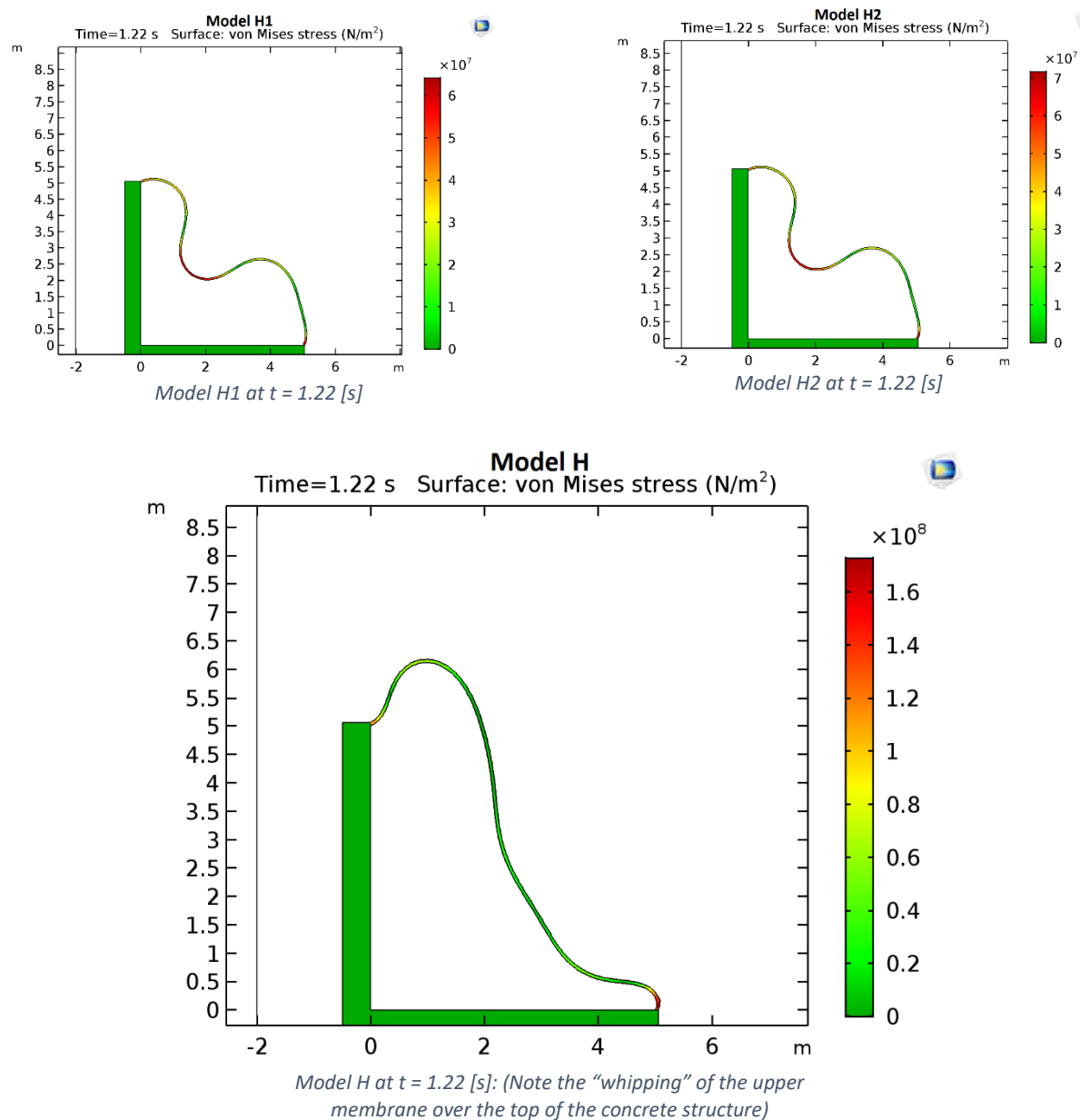
$$P = (ATM [Pa]) + (RhoSea [kg/m^3]) * (G [m/s^2]) * (Depth [m] - (y) [m])$$



Here the variable y represents the y-coordinate of the geometry the load is being applied to; in this case the external edge of the membrane. COMSOL will now apply a load perpendicular to the membrane as a function of the depth. Note that the “deepest” part of the membrane lies along the y-axis, meaning that at its lowest point ($y = 0$), the max pressure will be a function of the max depth; this means *Depth* should equal the depth of the lowest point of the membrane, not the lowest point of the system including the structure.

The efficacy of adding an accurate representation of the hydrostatic pressure gradient towards optimizing the eventual output simulation is high. This can be seen best when comparing 'Model H2' with 'Model H' ('Appendix A' and images below). In 'Model H2' (downwards pressure), the initial deformations occur at the top corner of the

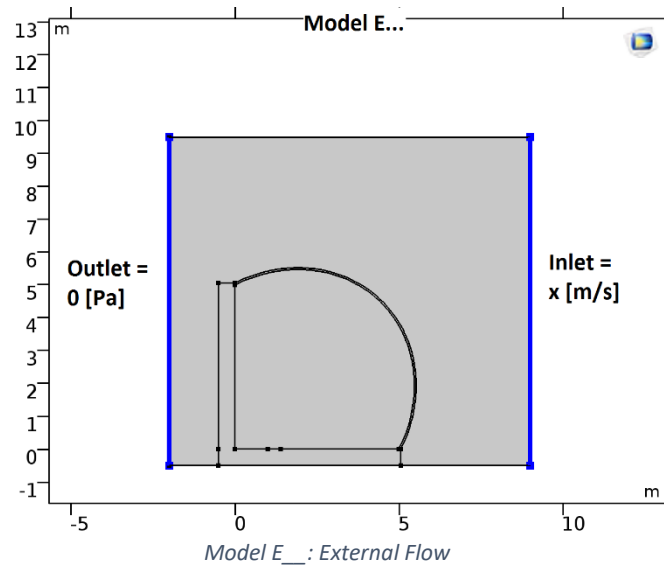
membrane, whereas in ‘Model H’ (varying boundary load), the initial deformations occur at the opposite corner. Furthermore, when subjected to hydrostatic pressure, the membrane has a tendency to “whip” over the top of the concrete structure (check *fig. Model H* below) When referencing the system description represented by *fig. X*, we see that this is due to the forces at the bottom of the membrane being greater than those at the top, meaning that ‘Model H’ models the true physical phenomena more accurately than ‘Model H2’. Though adding a varying boundary load (‘Model H’) increases computation time by 7.4%, this will be considered a necessary evil in order to get the most accurate simulation of the deformation behavior possible.



It is interesting to note that applying a non-varying boundary load ('Model H1') actually decreases the computational time by 10% when compared to a model with a prescribed pressure inlet ('Model H2'), most likely because COMSOL doesn't have to continuously recalculate the local pressure (magnitude and direction) for each time step throughout the entire Seawater Domain. Though as previously discussed, a non-varying boundary load doesn't lead to the most accurate results due to the oversimplification of reality, it has potential to decrease the computational load for future simulations that do not necessarily need the most accurate modelling of the membrane movement. However, because this project is highly interested in the deformation behavior, the most accurate model will be selected, 'Model H', and the varying-boundary load is applied to all further models.

External Flow

The updated 'Original Model A' now has a pressure-based outflow and an accurate hydrostatic pressure loading. An assumption made by the 'Original Model A' is that the Seawater domain is initially static; the influence of potential underwater currents is ignored. As determined in the 'Literature Review', underwater currents exist almost everywhere around the planet and typically range from 0 [m/s] to 4 [m/s], with 0.25 [m/s] being the average horizontal velocity. In order to model this naturally occurring phenomena, changes are made to the 'Original Model A'. This is achieved by changing the boundary conditions on the left and right of the Seawater Domain from two "Wall(s)" to a pressure-based outflow (at 0 [Pa]) and prescribed normal velocity inflow (at X [m/s]) respectively. This will allow the Seawater to flow freely through the system, depending on the velocities assigned to each boundary. Using a prescribed velocity is acceptable in this situation, as the force it exerts on the membrane is not a function of anything other than the acceleration it is hitting the membrane with. 'Model E' is created.

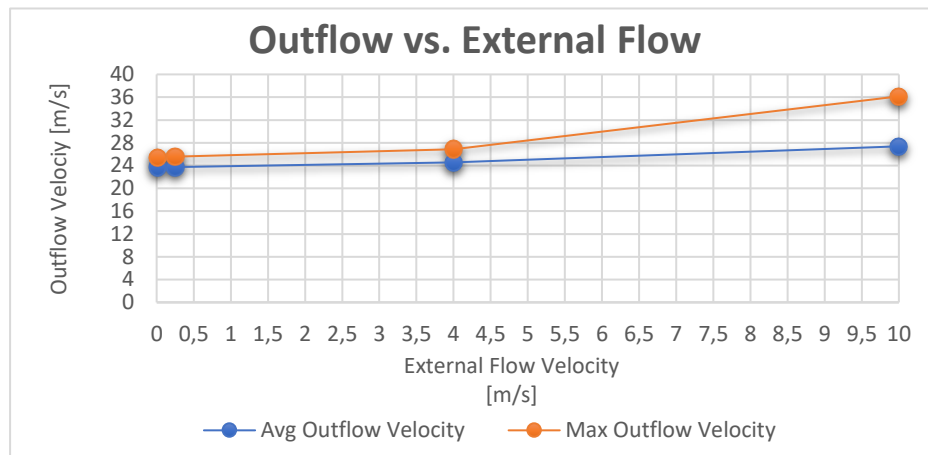


In order to determine the efficacy of adding the External Flow complexity to the model, it must be determined if the effects of adding these boundary conditions will make a noticeable difference or not. Identical models with varying inflow velocities and depths will be constructed and compared. The efficacy will be determined by observing the deformation behavior, measuring the resultant outflow velocity over time, and comparing computational time for each model. The table below makes this experiment a little more orderly. Note that all external flows are in the negative x-direction, as these flows will have the greatest potential effect on the deformation behavior.

		INPUT			OUTPUT			
		External Flow [m/s]	Depth [m]	Time Range (Start, Interval, End) [s]	Membrane Deformation Behavior	Computation Time [s]	Avg. Outflow [m/s]	Max Outflow [m/s]
Model Name	Model E1	0	40	(0,0.01,1.5)	Initial deformations in lower half of membrane. This causes the upper half of the membrane to "whip" over the top of the concrete. Phenomenon increases with external velocity.	323	23.71	25.42
	Model E1.1	0.01				324	23.74	25.44
	Model E2	0.25				343	23.74	25.59
	Model E3	4				325	24.55	26.85
	Model E3.1	8				565	27.38	36.15

Correlations to External Flow Velocity:

	<i>External Flow Velocity</i>
External Flow Velocity	1
Avg. Outflow Velocity	0.983762441
Max Outflow Velocity	0.961249196
Computation Time	0.905544287

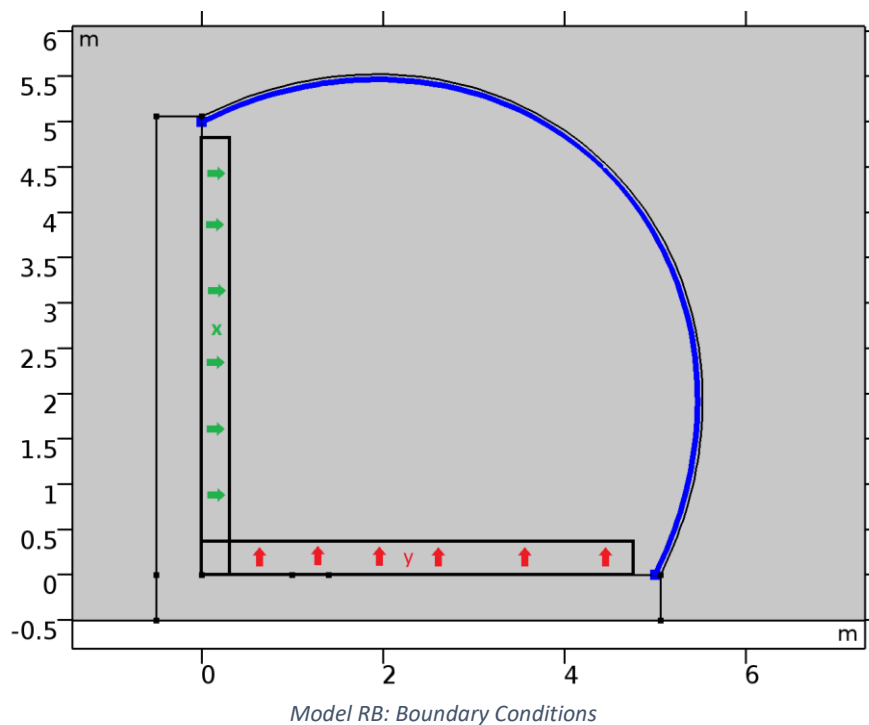


As seen in the correlation table above, the External Flow Velocity has strong correlation to both the Average Outflow velocity and the Maximum Outflow Velocity. Such a high correlation implies that outflow state is very much dependent on the External Flow Velocity; this leads us to the conclusion that it is indeed appropriate to consider external flow as an important piece of added complexity that will be incorporated in the final model. Furthermore, from the Outflow vs. External Flow scatter plot we observe that increasing the External Flow Velocity has a greater effect on the Max Outflow Velocity than it does on the Average Outflow Velocity; this can most likely be explained by the exaggerated deformation behavior (due to the horizontal external flow) creating pockets of fluid which lead to a more variable range of Outflow Velocity.

The correlation between Computation Time and External Flow Velocity is somewhat smaller but still positive; though this implies a definite increase in computational time given versus a model with a null External Flow Velocity, accuracy of the deformation behavior and resultant Outflow Velocities are of paramount importance, and therefore we can consider adding External Flow (to the output model) to be a sensible decision.

Reverse Boundary Spring Load

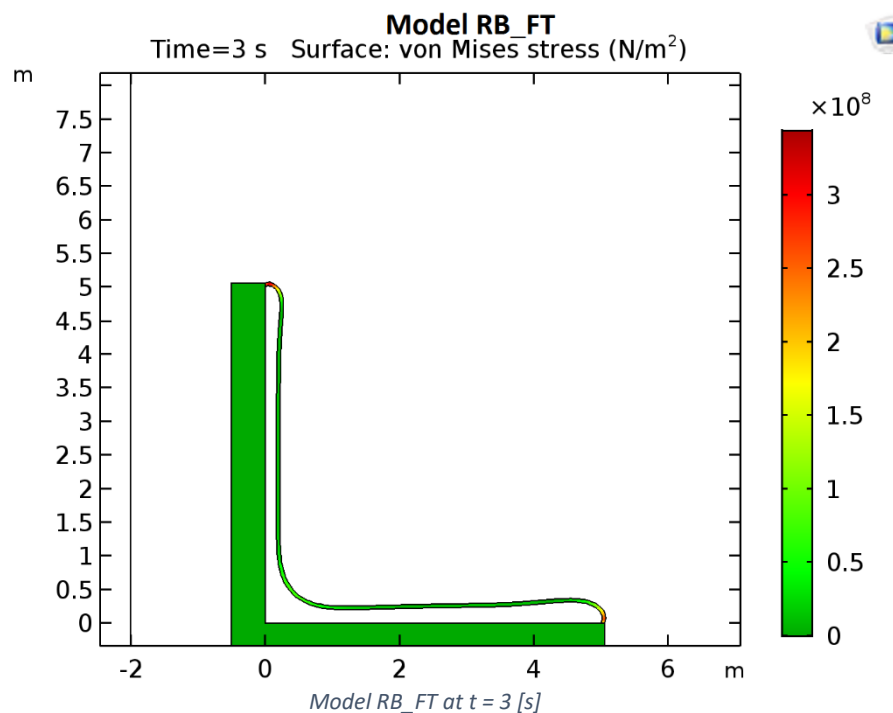
An unforeseen problem was encountered when running the (previous) simulations. Each previous simulation in the preceding sections was assigned a time range (to deform) that did not capture the full discharge time of the bladder. Because the Fluid Structure Interaction Multiphysics node was used in COMSOL, one of the first steps taken in defining a model was specifying the separate domains (Water/Seawater/EPDM/Concrete). Because COMSOL preforms simultaneous calculations of the relevant physics based on the domain it is analyzing, it is very important that each Domain stays fully separate and the number of Domains at the start of the simulation should stay the same throughout (COMSOL, 2017). However, because the bladder will always eventually touch the concrete Domain during deformation, this contact point has the undesired effect of splitting the Water Domain (inside the bladder) into two separate Domains; something which COMSOL is unable to process during a simulation. This is why all the time ranges (until this point) have been selected in a way that ensures that the simulation will end before contact occurs. After attempting and failing to create a “Contact Pair” between the flexible membrane and the concrete structure (impossible due to Water Domain separating them), the decision was made to apply a reverse boundary spring load applied to the inside of the membrane.



Along the highlighted blue boundary, a “Boundary Load” is assigned (which becomes active in the red and green sections), with the following equation:

Pressure =	$(x < .25) * (.25 - x) * (y < 4.8) * 10000000$	x	[N/m ²]
	$(y < .25) * (.25 - y) * (x < 4.8) * 10000000$	y	

Each point on this boundary will be continuously evaluated during the simulation, and if the membrane crosses either $x = .25$ or $y = .25$, a spring load of the form $F = K * x$ is applied. K is an arbitrarily selected spring constant, with the only condition being that K must large enough to ensure that a force greater than the force exerted by the Hydrostatic Pressure is present between $(0 < x < 0.25)$ and $(0 < y < 0.25)$. Note that an additional constraint is added into each equation ($y < 4.8$ on the x axis for example); this ensures that no force will be applied to either end of the flexible membrane, as these parts of the membrane would always be captured by the area in which the reverse boundary load is applied. If we wish to imagine how this would change the physical system, the reverse boundary spring load could be seen as a sort of frictionless metal grate raised 0.25 [m] from the concrete, fixed to the concrete with a spring. The permeable grate would allow for the water to discharge through it but prevent the membrane from touching the walls. ‘Model RB_FT’ below shows the final discharged state given the conditions.

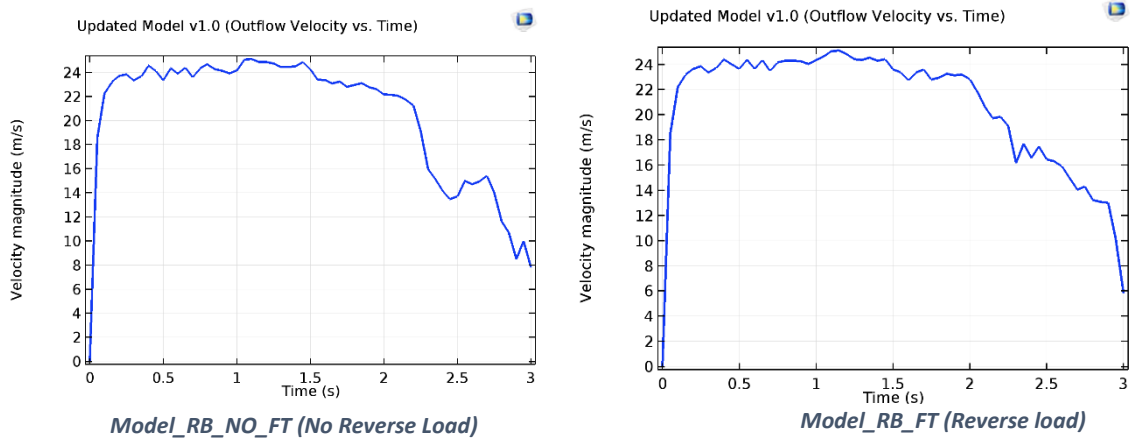


The efficacy of adding this extra complexity will be determined by running the following models:

		INPUT				OUTPUT			
		External Flow [m/s]	Depth [m]	Time Range (Start, Interval, End) [s]	Reverse Boundary Load?	Membrane Deform. Behavior	Computation Time [s]	Avg. Outflow [m/s]	Max Outflow [m/s]
Model Name	Model RB	0.25	40	(0,0.01,2.5) <i>(range < t_{critical})</i>	Yes	Membrane deforms until $x=0.25$ and $y=0.25$	705	23.69	25.35
	Model RB_NO				No	Membrane doesn't touch concrete	893	23.81	25.5
	Model RB_FT			(0,0.01,3.25) <i>(range > t_{critical})</i>	Yes	Membrane deforms until $x=0.25$ and $y=0.25$	1649	21.07	25.12
	Model RB_NO_FT				No	Membrane touches @ $t=3.09$ [s]	1797	20.83	25.5

‘Model RB’ and ‘Model RB_NO’ are run through identical simulations with the only difference being that ‘Model RB’ has a reverse boundary load and ‘Model RB_NO’ does not. As expected, in ‘Model RB’ the membrane is unable to deform past the $x = 0.25$ or $y = 0.25$. ‘Model RB_NO’ deforms as it normally would. When comparing the outflow velocities, both the Max Outflow and Avg. Outflow of ‘Model RB_NO’ (no reverse boundary load) are slightly higher than that of ‘Model RB’ (reverse boundary load). This makes sense, as we have set a variable load working in the opposite direction of the boundary load representing the hydrostatic pressure. Because the reverse boundary spring load does not allow for the full range of deformation possible, and effectively cuts out a chunk of the Maximum Potential Energy the system can hold, the average outflow velocity is expected to decrease by some amount.

‘Model RB_FT’ and ‘Model RB_NO_FT’ are given sufficiently large simulation time ranges, 0 [s] to 3 [s], in order to ensure that a situation with contact occurs (if there is no reverse boundary load). In ‘Model RB_NO_FT’, the membrane touches the concrete wall at $t = 3.09$ [s] = $t_{critical}$, stopping the simulation. When comparing plots of the outflow velocity versus time (graphs below), we see that there is a significantly larger drop in outflow velocity at $t = 2.2$ [s] for ‘Model RB_NO_FT’ (no reverse load) than for ‘Model RB_FT’. The average percentage relative error regarding outflow velocity versus time of ‘Model RB_FT’ versus ‘Model RB_NO_FT’ is 5.54 [%] given the full time range. Furthermore, when looking at the table, it is noted that ‘Model RB_FT’ (reverse load) has a higher average velocity but a lower maximum outflow velocity. Though initially this may seem counterintuitive, as in the previous experiment (‘Model RB’ vs ‘Model RB_NO’), ‘Model_RB’ had both a lower maximum and lower average outflow velocity, this can be explained by the fact that both ‘Model ..._FT’s have a time range that captures the contact time step. ‘Model RB_FT’ is able to discharge almost all of its Water Domain (until $x = 0.25$ and $y = 0.25$), whereas ‘Model RB_NO_FT’ cannot calculate outflow velocity after contact with the cement wall.

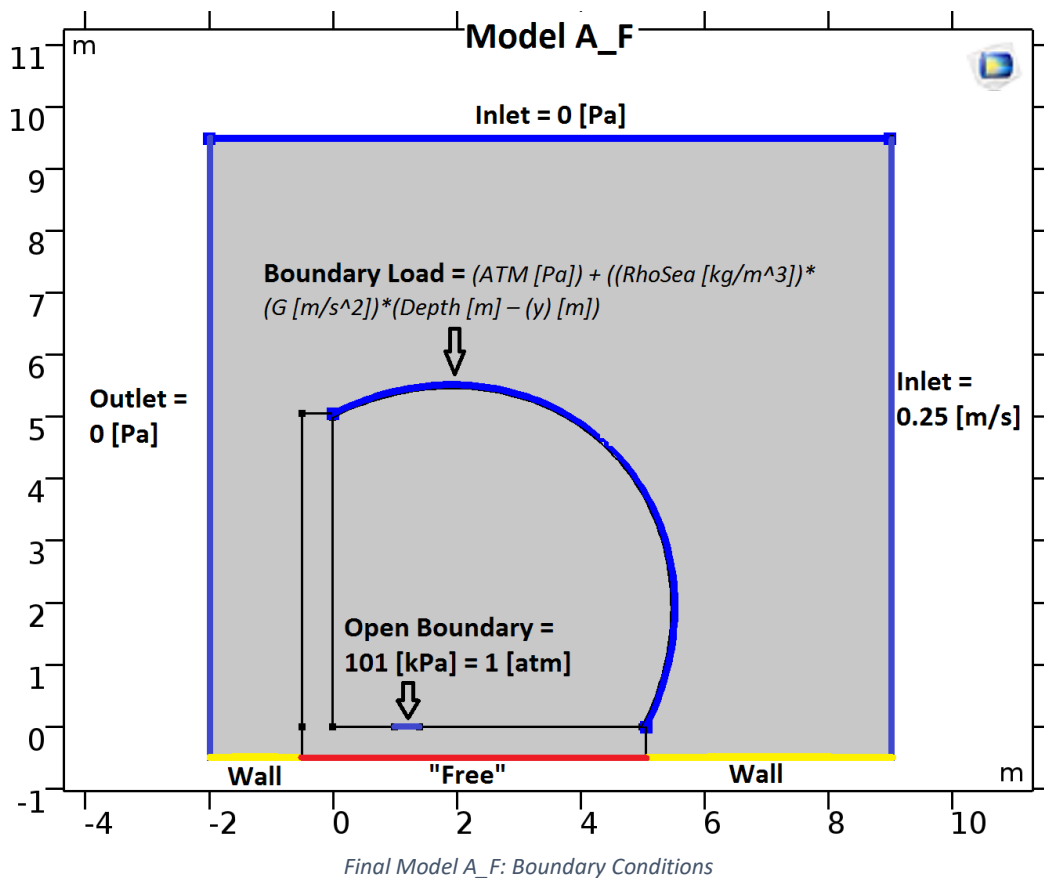


Based on this, and on the outflow velocity versus time plots, it can be concluded that adding a reverse boundary spring load will reduce the amount of variation of outflow velocity; this is why the maximum outflow velocity is always lower for a model with a reverse boundary load versus one without a reverse boundary load. A model with a reverse boundary load will have a higher average outflow velocity if its $range > t_{critical}$, when $t_{critical}$ = the time at which a model (without a reverse boundary load) would make contact with a wall. A model with a reverse boundary load will have a higher relative computational time if $range < t_{critical}$ and will have a lower relative

computational time if $range > t_{critical}$. Based on these observations, the decision is made to *not* include this working principle (reverse boundary load) to the final model used in “further analysis”. Because all further simulations will be run in a time $range < t_{critical}$, the loss of accurate outflow velocity variations (average percentage relative error = 5.54%) and additional computational cost make adding a reverse boundary load a sub-optimal design choice.

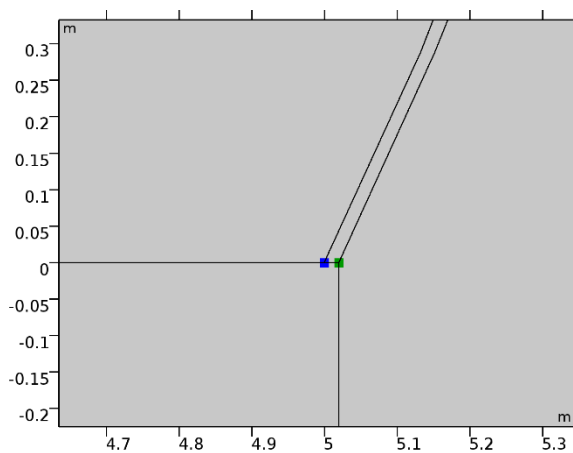
Further Analysis

‘Final Model A_F’ is created. This model includes all the working principles discussed previously other than the Reverse Boundary Spring Load, as all simulations will be run with time ranges too small for contact to be an issue. The effect of Membrane Thickness on the deformation behavior will be analyzed. The image below defines the boundary conditions assigned to the ‘Final Model A_F’.

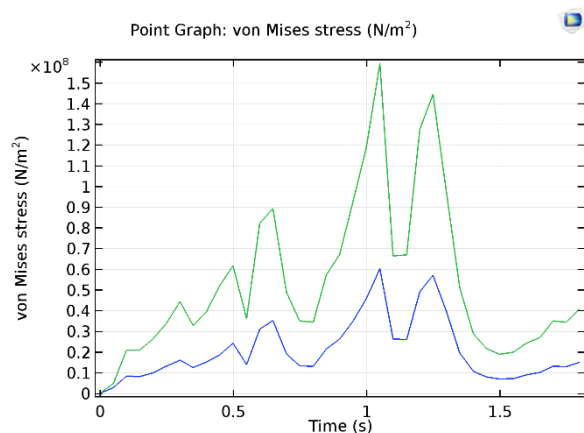


Membrane Thickness

Thus far, all simulations have been performed with the chosen membrane thickness of 60 [mm]. In order to determine the relationship between the flexible membrane's thickness and the deformation behavior, multiple identical models with varying membrane thickness are created. Von Mises stress has a local maximum at the bottom attachment point on the outside boundary of the membrane (as seen in images below), regardless of the membrane thickness. This is why all von Mises stress data has been extracted from this point. An overview of the simulations performed can be found below.



Final Model A_F: Stress Measurement Points, Lower Membrane attachment location



Final Model A_F: Stress Measurement Plot

		INPUT				OUTPUT				
		Ext. Flow [m/s]	Depth [m]	Time Range (Start, Interval, End) [s]	Membrane Thickness [mm]	Maximum von Mises Stress [N/m ²]	Average Von Mises Stress [N/m ²]	Comp Time [s]	Avg. Outflow [m/s]	Max Outflow [m/s]
Model Name	Model A_F20	0.25	40	(0,0.01,1.8) <i>range < t_{critical}</i>	20	1.6E8	5.47E7	2065	23.85	24.59
	Model A_F40				40	1.04E8	4.27E7	610	23.86	25.00
	Model A_F60				60	9.72E7	3.65E7	332	23.83	25.11
	Model A_F80				80	8.64E7	3.12E7	206	23.75	25.39
	Model A_F100				100	8.28E7	2.82E7	184	23.42	25.49

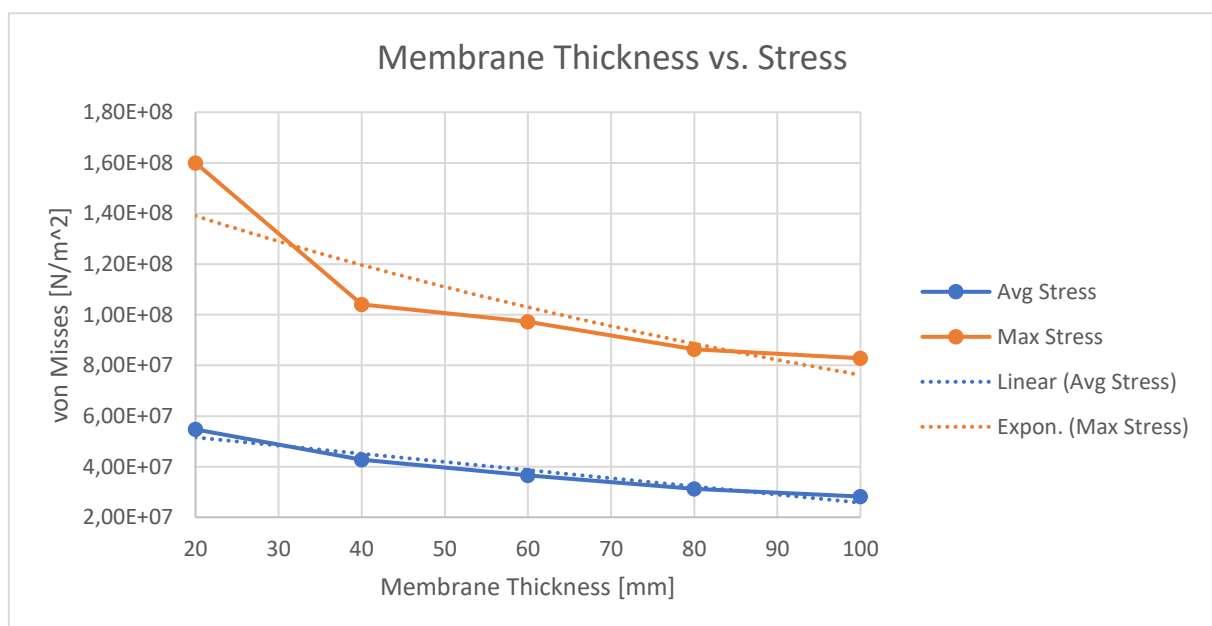
Correlations of Membrane Thickness & Outflow:

	<i>Membrane Thickness</i>
Membrane Thickness	1
Avg. Out	-0.8284
Max Out	0.1194

Based on the Correlation table found above, we reject the hypothesis that Maximum Outflow Velocity is linked to the Membrane Thickness. The Average Outflow Velocity has a medium to strong negative correlation with Membrane Thickness. It is important to note, however, that even though this correlation certainly exists, the factor with which the Membrane Thickness changes the Average Outflow Velocity is weak; a delta of 80 [mm] (= 80%) in Membrane Thickness gave a delta of just 0.44 [m/s] (= 1.84%). Based on this, the conclusion is made that Membrane Thickness has little effect on Outflow Velocity.

Correlations of Membrane Thickness & von Misses Stress:

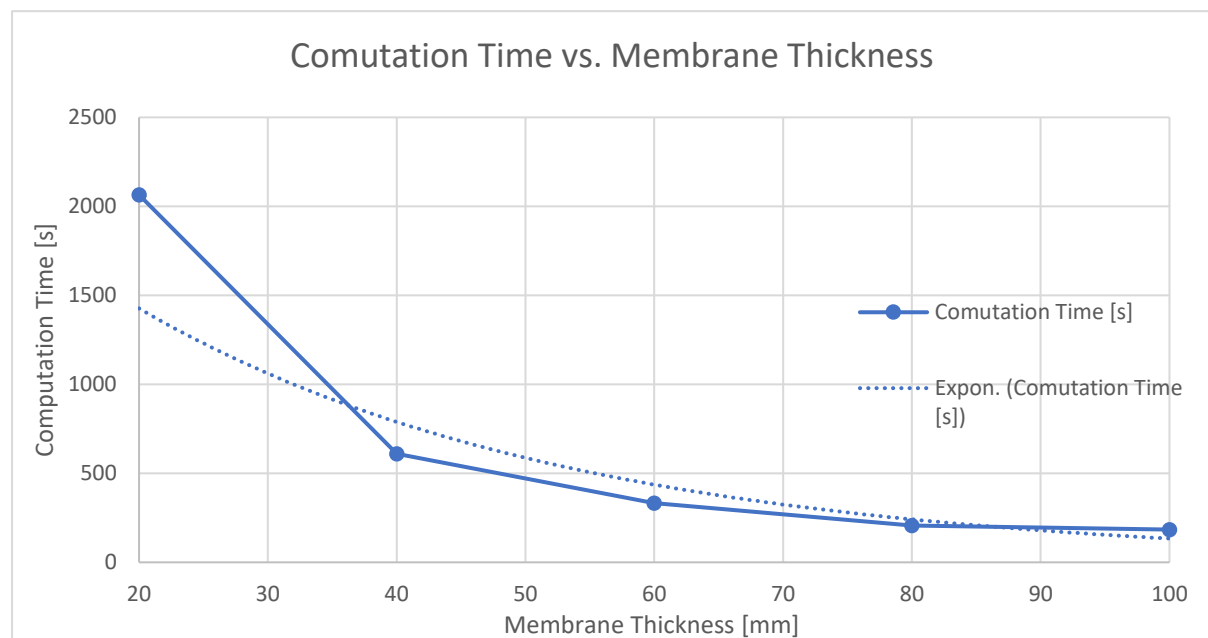
	<i>Membrane Thickness</i>
Membrane Thickness	1
Avg. Stress	-0.9687
Max Stress	-0.8687



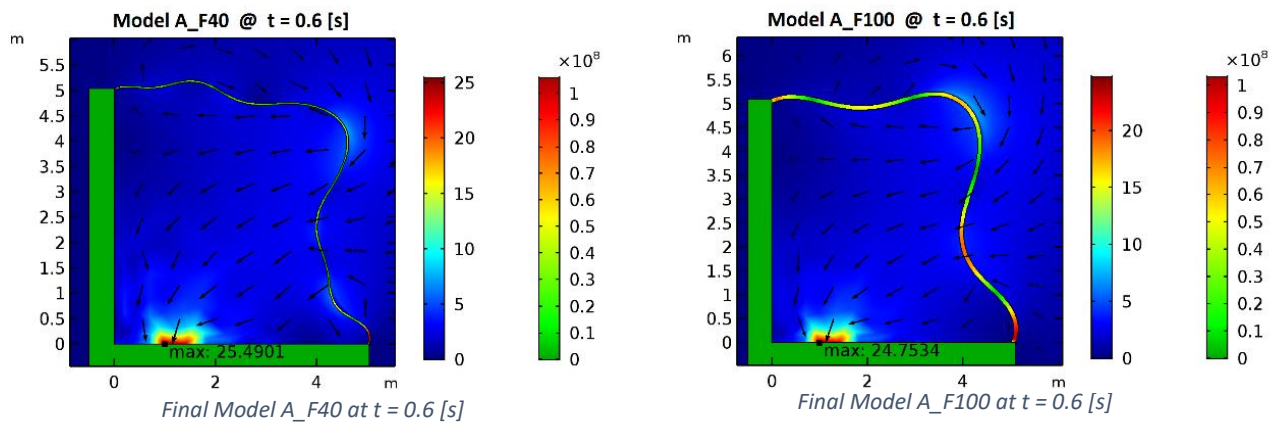
The correlation between Membrane Thickness and Stress is strong and negative. The Average Stress concentration has a near perfect linear relationship with Membrane Thickness; the Average Stress Concentration decreases by about $3.31\text{E}5 \text{ [N/m}^2\text{]}$ for every additional millimeter of Membrane Thickness. The Maximum Stress and Membrane Thickness also share a negative correlation, though somewhat weaker (less linear). When looking at the Membrane Thickness vs. Stress plot, we observe that Maximum Stress has a potentially non-linear relationship with Membrane Thickness, particularly when Membrane Thickness $< 40 \text{ [mm]}$. In order to make a more concrete decision about if the behavior is exponential or not, more data points (particularly with a smaller Membrane Thickness) should be collected and plotted. This was attempted but found to be impossible; the simulations would not converge past a minimum of 20 [mm] thickness, with all other parameters and settings being maintained identical for each simulation.

Correlations of Membrane Thickness & Computation Time:

	<i>Membrane Thickness</i> <i>[mm]</i>
Membrane Thickness [mm]	1
Computation Time [s]	-0.881

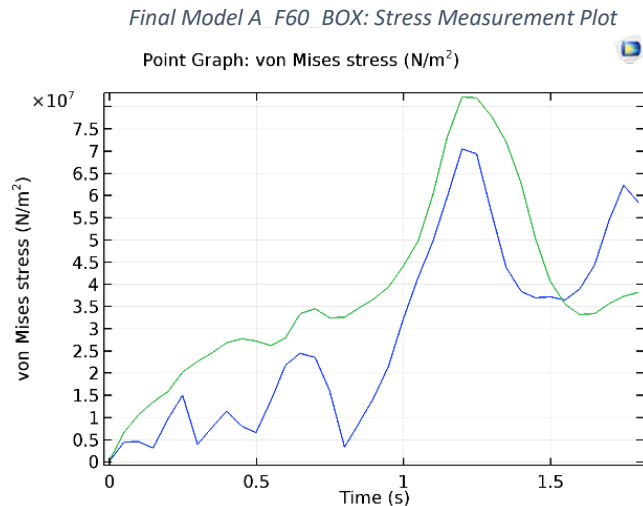
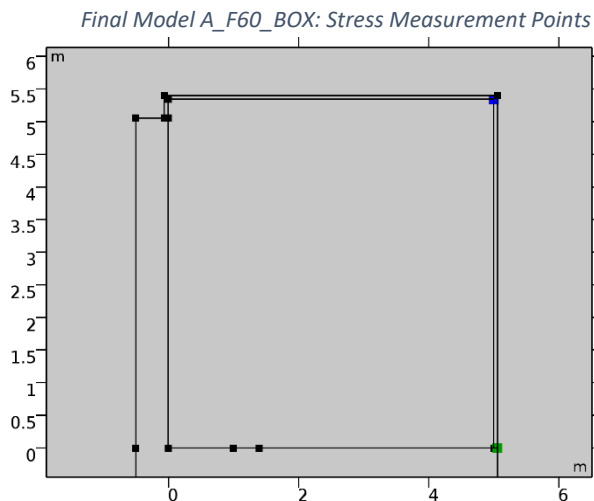


The correlation between Membrane Thickness and Computational Time is strongly negative. The relationship between these two parameters can be considered as Exponential, based on a visual interpretation of the Computational Time vs. Membrane Thickness plot (above). This is most likely due to the exponential increase in complexity of membrane deformation behavior versus membrane thickness. A thinner membrane is easier to deform, so the thinner the membrane is, the amount of small deformations in the membrane increases. This can be best seen in the images below (comparing Model A_F20 with Model A_F100). The more the membrane deforms, the more computational power is necessary to calculate the exact position of each point along the membrane.



Membrane Geometry

Until this point, all simulations have been run assuming the geometry defined by the 'Original Model A'. The potential effect of changing the basic geometric shape of the flexible bladder is now explored. Based on the literature search, the potential for a tubular (more rectangular) shape being more effective at storing potential energy is existing, and therefore the following simulation is run. The area of the water domain inside the bladder of Original Model A is equal to the area of the water domain inside the bladder of 'Model A_F60_BOX'. Furthermore, all other boundary conditions such as external flow, boundary loading, and membrane thickness are identical between the two models.



As seen in the images above, the point of maximum stress concentration for Model A_F60_BOX is determined to be in the same location (bottom outside edge) as in the previous simulations with the original membrane geometry.

		INPUT				OUTPUT				
		Ext. Flow [m/s]	Depth [m]	Time Range (Start, Interval, End) [s]	Mem. Thickness [mm]	Maximum von Mises Stress [N/m ²]	Average Von Mises Stress [N/m ²]	Comp Time [s]	Avg. Outflow [m/s]	Max Outflow [m/s]
Model Name	Model A_F60	0.25	40	(0,0.01,1.8) <i>Range < t_critical</i>	60	9.72E7	3.65E7	N/A	23.83	25.11
	Model A_F60_BOX					8.23E7	3.90E7	N/A	23.84	24.92

Based on the output of the experiment (table above), the following preliminary conclusions can be made. In 'Appendix B', the deformation of the membrane over time of 'Model A_F60_BOX' can be found. The Average Outflow Velocity and Maximum Outflow Velocity remain virtually unchanged between the two membrane shapes. 'Model A_F60' (regular shape) has a higher Maximum Stress along the flexible membrane, whereas the 'Model A_F60_BOX' has a higher Average Stress concentration. The reason for this occurrence is unknown, but the implications of this information will be explored in 'Conclusion'.

Discussion & Implications

Based on the findings in the “further analysis” and “adding working principles” section, the following conclusions can be made for future simulations and analysis.

The addition of the working principle Pressure-based Outflow is a necessary piece of added complexity to the model. Though it certainly increases the computational expense, it critically allows for analysis of outflow behavior (movement and velocity) over time. This specific piece of analysis is used multiple times during the research, and we can therefore consider the addition of a Pressure-based Outflow as something which will lead to a more optimal simulation model. The Hydrostatic Pressure Gradient is determined to be a key addition to the model, as the membrane deformation movement is inaccurate without its inclusion. Adding this physical phenomenon by means of a varying boundary load is ideal, as it reduces computational expense while simultaneously improving the correctness of the deformation movement. The inclusion of External Flow in the final model can be considered more optimal than a simulation without External Flow, as its inclusion allows the eventual output simulation to compute in a more realistic, dynamic environment. Furthermore, extreme cases such as the bladder being placed underwater near a river outlet (or any other place with a high underwater current) can now be modelled in future simulations. The average flow velocity of 0.25 [m/s] used in the previous research has a discernible effect on deformation movement and outflow velocity, though maybe not strong enough of an effect to warrant major design changes to the flexible reservoir. The Reverse Boundary Spring Load is deemed to be unnecessary for the final model output of this research, as all simulations were run in a time range that didn't capture the $t_{critical}$ (time at which contact would occur without boundary load). However, there may be a need to run the simulations past $t_{critical}$ in future analysis, and then it would be advisable to include the Reverse Boundary Load in order to prevent contact.

Because the membrane thickness has a relatively unpronounced effect on Outflow Velocity, and a rather pronounced effect on Computational Time, thin membranes should be avoided when performing simulations built to establish Outflow Velocity behavior (to calculate power, variation, etc.). However, if future simulations are made with the intention of extracting useful information about either the deformation behavior (movement) or stress concentrations within the bladder, the membrane

thickness will make a significant difference and cannot be arbitrarily increased to cut computational expense.

The main implications of the findings for the primary stakeholder are as follows. After discovering that the hydrostatic pressure will induce some sort of “whipping” effect (of the membrane), which in turn can extend the membrane past its steady-state full position, it may be prudent to consider creating a sort of safety-zone around the membrane. This safety-zone would not have any meaning in a physical sense but would set minimum space requirements for the flexible reservoir to deform freely, without running the risk of making contact with surrounding objects. Furthermore, though the addition of the Reverse Boundary Spring Load is a virtual operation to prevent contact in the simulation, the very real problem of the membrane making contact with the cement walls and/or being sucked into the outlet cannot be overlooked. Not only will this reduce the amount of effective potential energy that can be converted to electricity, it has the potential to induce mechanical failure (ripping of membrane due to friction with wall or membrane being sucked into turbine). The physical interpretation of the Reverse Boundary Spring Load, the lubricated metal grate fixed with springs (more detail in “Adding Working Principles” section), may actually be an effective way of preventing this from occurring.

The primary stakeholder can feel reasonably assured that while the underwater currents the flexible reservoir will likely experience (0 [m/s] to 4 [m/s]) will have some effect on its outflow velocity and membrane deformation movement, it will not affect the flexible reservoir in a way that will require design changes. Furthermore, the output velocity of the simulation is not affected in a meaningful way by changing the geometry of the flexible bladder. The stress concentrations are however affected, which has the following implications. If the bladder geometry is rectangular, the Average Stress at the point of maximum stress is higher, though the Maximum Stress is lower. This difference will influence the fatigue of the EPDM material over time, and further variation of membrane geometry should be explored in further simulations.

Summary

The research and findings are now summarized with direct answers to the posed ‘Research Questions’.

- *How is current simulation modelled? Which assumptions have been made?
How can the relevant physics incorporated in the current model be amended?*

The current (original) simulation is (incorrectly) modelled such that a prescribed outflow velocity causes the flexible bladder to deform. It is assumed that the water surrounding the bladder is static. The key missing relevant physics are the lack of a hydrostatic pressure gradient (which can be recreated with a varying boundary load), and the lack of a pressure-based outflow (which can be modelled with different boundary conditions).

- *What does its typical external environment consist of (that has the potential of influencing the membrane deformation behavior)?*

The typical environment of the flexible membrane is dynamic as thermohaline currents are found all over the world (Augustyn, 2018). These currents have both horizontal and vertical velocity components, but since the vertical velocity is extremely small, it will most likely have no influence on membrane deformation behavior and is therefore ignored. The typical underwater current horizontal velocities range from 0 [m/s] to 4 [m/s]. It is determined that this external flow velocity has a strong correlation to outflow velocity and brings the simulation model closer to a realistic environment.

- *How does varying membrane geometry influence the deformation behavior?*

Decreasing the membrane thickness will increase the average stress magnitude of the flexible bladder linearly, while increasing the maximum stress magnitude exponentially. Decreasing the membrane thickness leads to a higher number of smaller deformations in the bladder, increasing the computational expense. The outflow behavior (velocity) of the bladder can be considered weakly correlated to membrane thickness.

While maintaining the same bladder ‘volume’ (2D = area) and changing shape, there is evidence that varying the shape of the bladder can change the locations and magnitudes of stress concentration within the membrane. There is an inadequate

amount of experimental results to make conclusions about which shape is the most optimal for Ocean Grazer. However, the results we do have indicate that further research analyzing various membrane shapes has the potential of identifying a more optimal bladder geometry.

References

Anderson, D., 2002. *Reducing the Cost of Preventive Maintenance*, Johannesburg: Oniqua Enterprise Analytics.

Augustyn, A., 2018. *Encyclopedia Britannica: Seawater: Temperature Distribution*.

[Online]

Available at: <https://www.britannica.com/science/seawater/Temperature-distribution#ref540400>

[Accessed 8 March 2019].

C.D. de Jong, G. L. S. S. I. E., 2010. *Hydrography*. eBook (2nd) ed. Delft, the Netherlands: Delft University Press.

COMSOL, 2017. *What are the Navier-Stokes Equations?*. [Online]

Available at: <https://www.comsol.nl/multiphysics/navier-stokes-equations>

[Accessed 9 March 2019].

Elzen, S. v. d., 2018. *The Ocean Grazer: Designing a flexible underwater reservoir*, Groningen: University of Groningen: FSE.

Frei, W., 2014. *Modeling the Hydrostatic Pressure of a Fluid*. [Online]

Available at: <https://www.comsol.com/blogs/modeling-hydrostatic-pressure-fluid-deformable-container/>

[Accessed 5 March 2019].

Geertsema, A., 2019. *Meeting* [Interview] (6 June 2019).

Gordon, A. L., 2018. *Encyclopedia Britannica: Ocean Current*. [Online]

Available at: <https://www.britannica.com/science/ocean-current>

[Accessed 10 March 2019].

Mas, J., 2016. Tubular design for underwater compressed air energy storage. *Journal of Energy Storage*, 8(November), pp. 27-34.

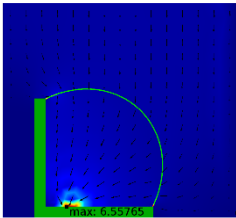
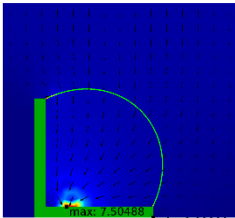
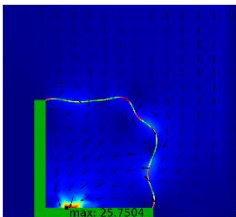
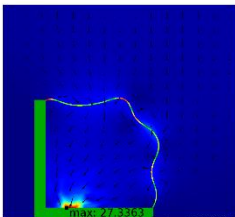
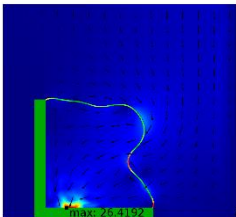
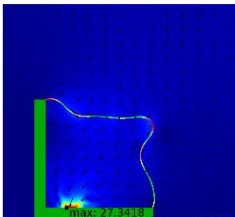
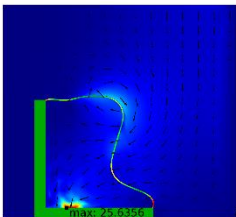
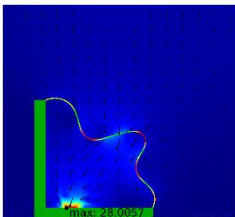
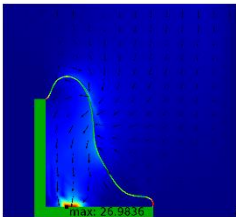
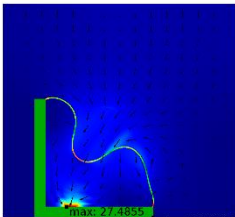
Rooij, M. v., 2019. *Question Session* [Interview] (22 March 2019).

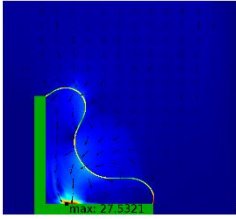
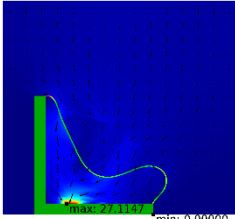
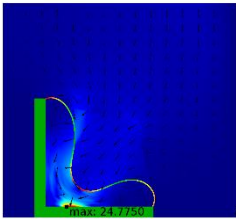
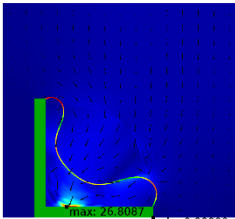
Vakis, A., 2015. Mechanical design and modeling of a single-piston pump for the novel power take-off system of a wave energy converter. *Renewable Energy*, 1(96), pp. 531-547.

Vakis, A., 2019. *Question Session #2* [Interview] (22 March 2019).

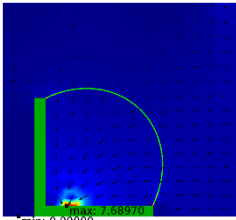
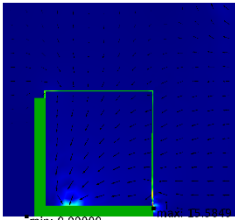
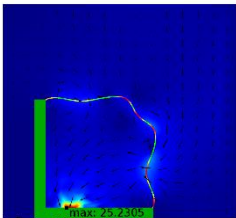
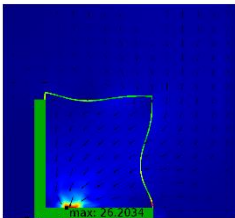
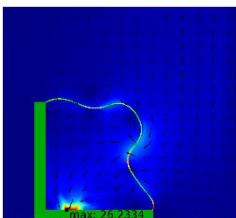
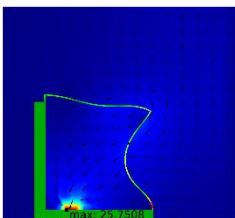
Appendix

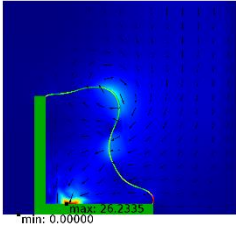
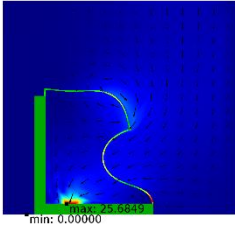
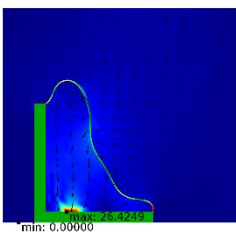
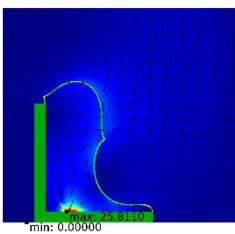
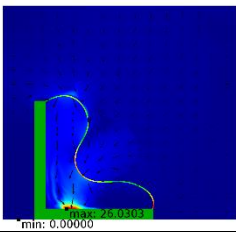
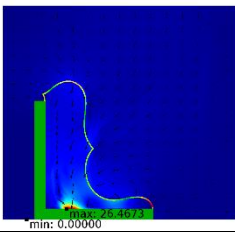
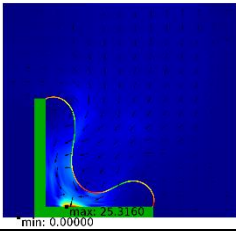
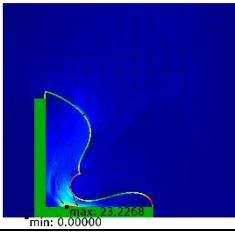
A. Working Principle: Hydrostatic Pressure Gradient

Time [s]	Model H (varying boundary load)	Model H2 (downwards pressure)
0.01	<p>Time=0.01 s Surface: von Mises stress (N/m²) Surface: Velocity magnitude (m/s) Arrow Surface: Velocity field (spatial frame) Max/Min Surface: Velocity magnitude (m/s)</p>  <p>max: 6.52765 min: 0.00000</p>	<p>Time=0.01 s Surface: von Mises stress (N/m²) Surface: Velocity magnitude (m/s) Arrow Surface: Velocity field (spatial frame) Max/Min Surface: Velocity magnitude (m/s)</p>  <p>max: 7.50486 min: 0.00000</p>
0.3	<p>Time=0.3 s Surface: von Mises stress (N/m²) Surface: Velocity magnitude (m/s) Arrow Surface: Velocity field (spatial frame) Max/Min Surface: Velocity magnitude (m/s)</p>  <p>max: 25.7505 min: 0.00000</p>	<p>Time=0.3 s Surface: von Mises stress (N/m²) Surface: Velocity magnitude (m/s) Arrow Surface: Velocity field (spatial frame) Max/Min Surface: Velocity magnitude (m/s)</p>  <p>max: 27.3256 min: 0.00000</p>
0.6	<p>Time=0.6 s Surface: von Mises stress (N/m²) Surface: Velocity magnitude (m/s) Arrow Surface: Velocity field (spatial frame) Max/Min Surface: Velocity magnitude (m/s)</p>  <p>max: 25.9352 min: 0.00000</p>	<p>Time=0.6 s Surface: von Mises stress (N/m²) Surface: Velocity magnitude (m/s) Arrow Surface: Velocity field (spatial frame) Max/Min Surface: Velocity magnitude (m/s)</p>  <p>max: 27.3256 min: 0.00000</p>
0.9	<p>Time=0.9 s Surface: von Mises stress (N/m²) Surface: Velocity magnitude (m/s) Arrow Surface: Velocity field (spatial frame) Max/Min Surface: Velocity magnitude (m/s)</p>  <p>max: 25.9352 min: 0.00000</p>	<p>Time=0.9 s Surface: von Mises stress (N/m²) Surface: Velocity magnitude (m/s) Arrow Surface: Velocity field (spatial frame) Max/Min Surface: Velocity magnitude (m/s)</p>  <p>max: 27.3256 min: 0.00000</p>
1.2	<p>Time=1.2 s Surface: von Mises stress (N/m²) Surface: Velocity magnitude (m/s) Arrow Surface: Velocity field (spatial frame) Max/Min Surface: Velocity magnitude (m/s)</p>  <p>max: 25.9352 min: 0.00000</p>	<p>Time=1.2 s Surface: von Mises stress (N/m²) Surface: Velocity magnitude (m/s) Arrow Surface: Velocity field (spatial frame) Max/Min Surface: Velocity magnitude (m/s)</p>  <p>max: 27.3256 min: 0.00000</p>

1.5	<p>Time=1.5 s Surface: von Mises stress (N/m²) Surface: Velocity magnitude (m/s) Arrow Surface: Velocity field (spatial frame) Max/Min Surface: Velocity magnitude (m/s)</p>  <p>min: 0.00000</p>	<p>Time=1.5 s Surface: von Mises stress (N/m²) Surface: Velocity magnitude (m/s) Arrow Surface: Velocity field (spatial frame) Max/Min Surface: Velocity magnitude (m/s)</p>  <p>min: 0.00000</p>
1.8	<p>Time=1.8 s Surface: von Mises stress (N/m²) Surface: Velocity magnitude (m/s) Arrow Surface: Velocity field (spatial frame) Max/Min Surface: Velocity magnitude (m/s)</p>  <p>min: 0.00000</p>	<p>Time=1.8 s Surface: von Mises stress (N/m²) Surface: Velocity magnitude (m/s) Arrow Surface: Velocity field (spatial frame) Max/Min Surface: Velocity magnitude (m/s)</p>  <p>min: 0.00000</p>

B. Further Analysis: Membrane Geometry

Time [s]	Model A_F60	Model A_F60_BOX
0.01	<p>Time=0.01 s Surface: von Mises stress (N/m²) Surface: Velocity magnitude (m/s) Arrow Surface: Velocity field (spatial frame) Max/Min Surface: Velocity magnitude (m/s)</p>  <p>min: 0.00000</p>	<p>Time=0.01 s Surface: von Mises stress (N/m²) Surface: Velocity magnitude (m/s) Arrow Surface: Velocity field (spatial frame) Max/Min Surface: Velocity magnitude (m/s)</p>  <p>min: 0.00000</p>
0.3	<p>Time=0.3 s Surface: von Mises stress (N/m²) Surface: Velocity magnitude (m/s) Arrow Surface: Velocity field (spatial frame) Max/Min Surface: Velocity magnitude (m/s)</p>  <p>min: 0.00000</p>	<p>Time=0.3 s Surface: von Mises stress (N/m²) Surface: Velocity magnitude (m/s) Arrow Surface: Velocity field (spatial frame) Max/Min Surface: Velocity magnitude (m/s)</p>  <p>min: 0.00000</p>
0.6	<p>Time=0.6 s Surface: von Mises stress (N/m²) Surface: Velocity magnitude (m/s) Arrow Surface: Velocity field (spatial frame) Max/Min Surface: Velocity magnitude (m/s)</p>  <p>min: 0.00000</p>	<p>Time=0.6 s Surface: von Mises stress (N/m²) Surface: Velocity magnitude (m/s) Arrow Surface: Velocity field (spatial frame) Max/Min Surface: Velocity magnitude (m/s)</p>  <p>min: 0.00000</p>

0.9	<p>Time=0.9 s Surface: von Mises stress (N/m²) Surface: Velocity magnitude (m/s) Arrow Surface: Velocity field (spatial frame) Max/Min Surface: Velocity magnitude (m/s)</p>  <p>min: 0.00000</p>	<p>Time=0.9 s Surface: von Mises stress (N/m²) Surface: Velocity magnitude (m/s) Arrow Surface: Velocity field (spatial frame) Max/Min Surface: Velocity magnitude (m/s)</p>  <p>min: 0.00000</p>
1.2	<p>Time=1.2 s Surface: von Mises stress (N/m²) Surface: Velocity magnitude (m/s) Arrow Surface: Velocity field (spatial frame) Max/Min Surface: Velocity magnitude (m/s)</p>  <p>min: 0.00000</p>	<p>Time=1.2 s Surface: von Mises stress (N/m²) Surface: Velocity magnitude (m/s) Arrow Surface: Velocity field (spatial frame) Max/Min Surface: Velocity magnitude (m/s)</p>  <p>min: 0.00000</p>
1.5	<p>Time=1.5 s Surface: von Mises stress (N/m²) Surface: Velocity magnitude (m/s) Arrow Surface: Velocity field (spatial frame) Max/Min Surface: Velocity magnitude (m/s)</p>  <p>min: 0.00000</p>	<p>Time=1.5 s Surface: von Mises stress (N/m²) Surface: Velocity magnitude (m/s) Arrow Surface: Velocity field (spatial frame) Max/Min Surface: Velocity magnitude (m/s)</p>  <p>min: 0.00000</p>
1.8	<p>Time=1.8 s Surface: von Mises stress (N/m²) Surface: Velocity magnitude (m/s) Arrow Surface: Velocity field (spatial frame) Max/Min Surface: Velocity magnitude (m/s)</p>  <p>min: 0.00000</p>	<p>Time=1.8 s Surface: von Mises stress (N/m²) Surface: Velocity magnitude (m/s) Arrow Surface: Velocity field (spatial frame) Max/Min Surface: Velocity magnitude (m/s)</p>  <p>min: 0.00000</p>

C. “Optimality”

	Model Validity	Influence on Deform. Behavior	Reduce Computational Expense	= Optimality	FINAL MODEL
Working Principle “X”	x1	x2	x3	$x1 + x2 + x3 = \text{Opt.}$	Yes if Opt. > 0

- ▶ Model Validity, $x1 = [2, -2]$:
 - ▶ 2 if working principle “X” brings simulation boundary conditions closer to reality
 - ▶ -2 if working principle “X” brings simulation boundary conditions further from reality
- ▶ Influence on Deformation Behavior, $x2 = [0, 2]$: Average % rel. error (versus original) of outflow velocity vs. time.
 - ▶ 2 = Average % rel. error $\geq 1\%$
 - ▶ 1 = Average % rel. error $< 1\%$
 - ▶ 0 = Average % rel. error $\approx 0\%$
 - ▶ Note: given positive values [0,2] only as it is assumed any differences in % rel. error (due to adding relevant working principle) contributes to a better model
- ▶ Reduce Computational Cost, $x3 = [-2, 2]$: Based on computation time
 - ▶ 2 = Comp. time decrease of $\geq 10\%$
 - ▶ 1 = Comp. time decrease of $\geq 0\%$
 - ▶ 0 = Comp. time decrease of $\approx 0\%$